Catalysis Today 158 (2010) 336–342

Contents lists available at ScienceDirect

Catalysis Today

journal homepage: www.elsevier.com/locate/cattod

# Low temperature catalytic combustion of chlorobenzene over Mn–Ce–O/γ-$Al_2O_3$ mixed oxides catalyst

Meng Wu, Xingyi Wang*, Qiguang Dai, Yaoxing Gu, Dao Li

*Research Institute of Industrial Catalysis, East China University of Science and Technology, Meilong Road 130, Shanghai 200237, China*

ARTICLE INFO

*Article history:*
Available online 14 May 2010

*Keywords:*
Chlorobenzene
$MnO_x$–$CeO_2$
$Al_2O_3$
Catalytic combustion
$CeO_2$

ABSTRACT

A series of $Mn_xCe_y/Al_2O_3$ mixed oxides catalysts with different compositions prepared by wet impregnation method were tested for catalytic combustion of chlorobenzene (CB), as a model of volatile organic compounds of chlorinated aromatics. $Mn_xCe_y/Al_2O_3$ mixed oxides catalysts present high activity for the low temperature catalytic destruction of CB and $Mn_8Ce_2/Al_2O_3$ catalyst is identified as the most active catalyst, on which the temperature of complete combustion of CB is 338 °C. Effects of systematic variation of reaction conditions, including space velocity and inlet CB and oxygen concentration on the reaction were investigated. Additionally, the stability and deactivation of $Mn_xCe_y/Al_2O_3$ mixed oxides catalysts were studied by various characterization methods and other assistant experiments. $Mn_xCe_y/Al_2O_3$ mixed oxides catalysts with high Mn/Ce ratios present a stable high activity, which is related to their better reducibility.



## 1. Introduction

Chlorinated volatile organic compounds (CVOCs) in waste gases are released to the atmosphere from a wide range of industrial processes or the incineration of municipal and medical wastes. Direct thermal combustion, a conventional technology for the destruction of chlorinated organic compounds usually requires temperatures higher than 850–1000 °C and leads to the formation of small amounts of toxic polychlorinated aromatic compounds (i.e., polychlorinated dibenzodioxins [PCDDs] and dibenzofurans [PCDFs]), in addition to the standard products (i.e., CO, $NO_x$, $SO_x$) from combustion. Therefore, stringent environmental regulations are in place in several countries limiting PCDD/PCDF emissions [1].

So far as we are concerned, the catalytic oxidation of CVOCs to carbon dioxide, HCl, and water is the best method for their destruction. The major advantage of the catalytic combustion is that oxidation can be efficiently performed at temperatures between 250 and 550 °C and very dilute pollutants which cannot be thermally combusted without additional fuel can be treated efficiently. Therefore, a low temperature catalytic combustion process offers significant cost saving when compared with the conventional thermal process.

Of studies of the catalysts for CVOC catalytic combustion, most have been reported focusing on the three types of catalysts based on noble metals [2,3], transition metals [4,5] or zeolites [6,7]. Metal catalysts have been widely used because of their ability to catalyze oxidation, but they are susceptible to the deactivation by HCl and $Cl_2$. The activities of zeolite are related to their acid properties. However, the problem of the formation of the by-product polychlorinated compounds on these catalysts is yet to be solved. Therefore, the development of catalysts having high performance in converting CVOCs is of great interest.

In our previous work [8,9], $CeO_2$ as a catalyst for CVOCs catalytic combustion was discussed, and its activity was found higher than that of other reported catalysts [10–14], but $CeO_2$ deactivated quickly due to strong adsorption of HCl or $Cl_2$ produced from the decomposition of CVOCs on the surface to blockade the active sites. However, it is found if chlorine or chloride ions adsorbed on the surface were removed or transferred rapidly enough, the stability of $CeO_2$ catalyst could be improved.

Among the catalysts for CVOCs catalytic combustion, including noble metals, transition metal oxides or solid acid catalysts, the transition metal oxide catalysts can resist the deactivation caused by chlorine poisoning. Manganese oxides, either supported or unsupported, were used as important catalysts directly in the catalytic reactions [15–19], such as the oxidation of carbon monoxide, methane and hydrocarbons, the decomposition of ozone, $N_2O$ and $H_2O_2$, and the selective catalytic reduction (SCR) of NO. The presence of Mn in Mn–Ce–O or Mn–Cu–O mixed oxide catalysts can enhance their catalytic activities for CO oxidation and SCR of NO.

In the present work, γ-$Al_2O_3$ supported mixed oxide catalysts, $Mn_xCe_y/Al_2O_3$, prepared by impregnation method, were tested in catalytic combustion of chlorobenzene (CB), and the effects of Mn amount in catalysts, operation conditions, such as space velocity

* Corresponding author. Tel.: +86 21 64253372; fax: +86 21 64253372.
*E-mail addresses:* wangxy@ecust.edu.cn, wangxy1958@yahoo.com.cn (X. Wang).

0920-5861/$ – see front matter © 2010 Elsevier B.V. All rights reserved.
doi:10.1016/j.cattod.2010.04.006

and inlet CB and oxygen concentration on catalytic activity were investigated. Additionally, the possible cause of catalyst deactivation was discussed based on the data from stability of $Mn_xCe_y/Al_2O_3$ catalysts and thus further investigated by assistant experiments.

## 2. Experimental

### 2.1. Catalysts preparation

A series of $Mn_xCe_y/Al_2O_3$ catalysts were prepared by incipient wetness impregnation. The aqueous solutions of $Mn(NO_3)_2$ and $Ce(NO_3)_3{\cdot}6H_2O$ (Sinopharm Chemical Reagent Corpration, 99.0%) were used as precursors. γ-$Al_2O_3$ support (surface area, 188 $m^2/g$; grain size, 20–40 mesh) was impregnated to incipient wetness with appropriate amounts of precursor aqueous solution with different Mn/Ce ratio. The impregnated solids were dried at 110 °C for 12 h and calcined at 550 °C for 4 h in air. The weight ratio of Mn plus Ce to γ-$Al_2O_3$ was 15%. In the text or figures, *x* and *y* in $Mn_xCe_y/Al_2O_3$ indicate the mole proportion of Mn and Ce, respectively. For example, $Mn_8Ce_2/Al_2O_3$ represents the catalyst with the Mn/Ce ratio of 8:2.

### 2.2. Catalyst characterization

#### 2.2.1. Powder X-ray diffraction

The powder X-ray diffraction patterns (XRD) of the samples were recorded on a Rigaku D/Max-rC powder diffractometer using Cu Kα radiation (40 kV and 100 mA). The diffractograms were recorded within the 2θ range of 10–80° with a 2θ step size of 0.02° and step time of 0.1 s.

#### 2.2.2. Nitrogen adsorption/desorption

The nitrogen adsorption and desorption isotherms were measured at −196 °C on an ASAP 2400 system in static measurement mode. The samples were outgassed at 160 °C for 4 h before the measurement. The specific surface area was calculated using the BET model.

#### 2.2.3. Thermogravimetric analysis

Coke formation on the catalyst was evaluated with thermogravimetric analysis (TGA) using a PerkinElmer Pyris Diamond TG/TGA Setaram instrument. The fresh and used $Mn_xCe_y/Al_2O_3$ samples were heated up to 800 °C from room temperature (heating rate of 10 °C/min) in a $N_2/O_2$ stream.

#### 2.2.4. X-ray photoelectron spectroscopy

The XPS measurements were made on a VG ESCALAB MK II spectrometer by using Mg Kα (1253.6 eV) radiation as the excitation source. Charging of samples was corrected by setting the binding energy of adventitious carbon (C1s) at 284.6 eV. The powder sample, pressed in the form of self-supporting disks, was loaded in a sub-chamber and then evacuated for 4 h prior to the measurements at 25 °C.

#### 2.2.5. Temperature programming reduction

$H_2$-temperature programming reduction ($H_2$-TPR) was investigated by heating $Mn_xCe_y/Al_2O_3$ samples (100 mg) in $H_2$ (5 vol.%)/Ar flow (30 ml/min) at a heating rate of 10 °C/min from 20 to 750 °C. The hydrogen consumption was monitored by thermoconductivity detector (TCD). Before $H_2$-TPR analysis, the sample was heated for 60 min in Ar flow at 500 °C, and then treated in $O_2$ at room temperature for 30 min.

#### 2.2.6. Raman spectroscopy

The Raman spectra were obtained on a Renishaw in Viat + Reflex spectrometer equipped with a CCD detector at ambient temperature and moisture-free conditions. The emission line at 514.5 nm from an $Ar^+$ ion laser (Spectra Physics) was focused, analyzing spot about 1 μm, on the sample under the microscope. The power of the incident beam on the sample was 3 mW. Time of acquisition varied according to the intensity of the Raman scattering. The wavenumbers obtained from spectra were accurate to 2 $cm^{-1}$.

### 2.3. Catalytic activity measurement

Catalytic combustion reactions were carried out at atmospheric pressure in a continuous flow micro-reactor made of a quartz tube of 4 mm in inner diameter. Two-hundred milligram catalyst (grain size, 20–40 mesh) was packed at the bed of the reactor. The feed stream to reactor was therefore prepared by delivering liquid CB with a syringe pump into dry air, which was metered by a mass flow controller. The injection point was electrically heated to ensure the complete evaporation of CB. The feed flow through the reactor was set with the concentration of CB 1000 ppm and the gas hourly space velocity (GHSV) at 15,000 ml/g h. The temperature of reaction was measured and controlled with a thermocouple located just at the hot spot of the reactor bed. The effluent gases were analyzed on-line at a given temperature by using two gas chromatographs (GC), one equipped with FID for organic chlorinated reactant, and the other with TCD for CO and $CO_2$. The concentrations of $Cl_2$ and HCl were analyzed by the effluent stream bubbling through a 0.0125N NaOH solution, and chlorine concentration was then determined by the titration with ferrous ammonium sulphate (FAS) using N,N-diethyl-p-phenylenediamine (DPD) as indicator [20]. The concentration of chloride ions in the bubbled solution was determined by using a chloride ion selective electrode [21].

## 3. Results and discussion

### 3.1. Characterization

Wide angle XRD patterns of $Mn_xCe_y/Al_2O_3$ mixed oxides catalysts with different ratios of Mn/Ce are shown in Fig. 1. γ-$Al_2O_3$ support only exhibits three broad diffraction peaks at 36.9°, 45.9° and 66.6°, ascribed to spinal phase. The diffractogram of $CeO_2/Al_2O_3$ shows the diffraction peaks at 28.6°, 33.3°, 47.5°, 56.5° and 59.2° of cerianite characterized with a fluorite-like structure. Heavily asymmetric shape of such reflections with a lower

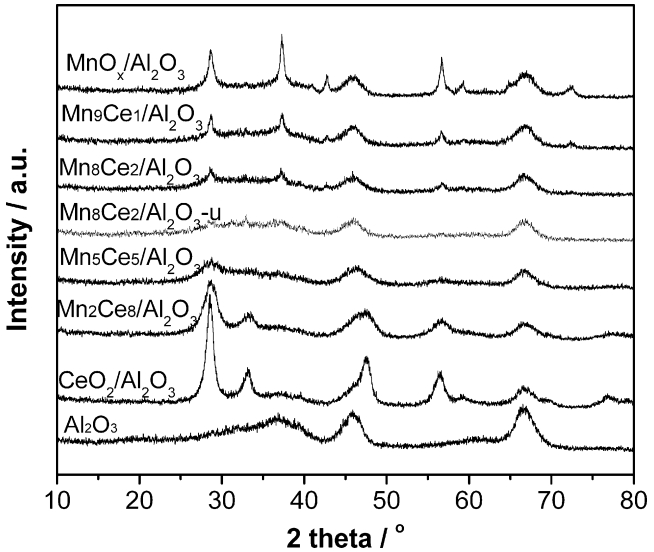


**Fig. 1.** XRD patterns of $Mn_xCe_y/Al_2O_3$ mixed oxides catalysts with different ratios of Mn/Ce; u, the used catalyst.

**Table 1**
The properties of $Mn_xCe_y/Al_2O_3$ mixed oxides catalysts.

| Catalysts | Mn/Ce (at.%/at.%)[a] | Mn (wt.%)[a] | Mn/Ce (at.%/at.%)[b] | Surface area ($m^2$/g) | $d_{1\,1\,1(CeO_2)}$ (Å) | $d_{CeO_2}$ (nm)[c] | $d_{MnO_2}$ (nm)[d] | O1s core level (eV) |
|---|---|---|---|---|---|---|---|---|
| $MnO_x/Al_2O_3$ | – | 15 | – | 141 | – | – | 16.9 | – |
| $Mn_9Ce_1/Al_2O_3$ | 9/1 | 11.7 | 4.57 | 159 | NT | NT | 9.8 | 531.0 |
| $Mn_8Ce_2/Al_2O_3$ | 8/2 | 9.2 | 2.34 | 135 | NT | NT | 7.0 | 531.7 |
| $Mn_5Ce_5/Al_2O_3$ | 5/5 | 4.2 | 0.97 | 118 | 3.0973 | 4.8 | NT | 532.1 |
| $Mn_2Ce_8/Al_2O_3$ | 2/8 | 1.3 | 0.23 | 136 | 3.1037 | 5.2 | NT | 531.8 |
| $CeO_2/Al_2O_3$ | – | 0 | 0 | 188 | 3.1164 | 10.5 | – | 531.1, 530.0 |

[a] From the components during the preparation.
[b] Estimated by XPS.
[c] From the Scherrer equation, applied to the [1 1 1] reflection of the cerianite.
[d] [1 0 1] reflection of the pyrolusite. NT, not detectable.

intensity confirms the weakening degree of the crystallinity of samples with Mn/Ce ratio from 0.25 to 4, which is consistent with the fact that small average particle size of ceria of $Mn_2Ce_8/Al_2O_3$ and $Mn_5Ce_5/Al_2O_3$ was calculated through the Scherrer equation, applied to the [1 1 1] reflection of cerianite. For $Mn_8Ce_2/Al_2O_3$ sample, the peak at 28.6° of [1 1 1] overlaps the peak at 28.7° of $MnO_2$ in the form of pyrolusite [22,23] so that it is difficult to estimate the size of ceria. A weak peak at 33.5° is observed, due to the diffraction from [2 0 0] of cerianite, indicating that the cerianite structure exists. It can be deduced that the size of ceria of $Mn_8Ce_2/Al_2O_3$ sample should be smaller than 4.8 nm, the size of $Mn_5Ce_5/Al_2O_3$ sample (Table 1). Therefore, the appreciable decrease in ceria particle size parallels with an increase in Mn amount.

Moreover, the diffraction peaks of cubic fluorite-like structure of $Mn_xCe_y/Al_2O_3$ mixed oxides catalysts shift to slightly higher values of Bragg angles from 28.7° to 29.0°, indicating that a part of manganese species can enter the fluorite lattice to form $MnCeO_x$ solid solutions [24]. As reported in Ref. [25], the ionic radius of $Mn^{3+}$ (0.066 nm) is smaller than that of $Ce^{4+}$ (0.094 nm), and the incorporation of $Mn^{3+}$ into the fluorite lattice results in the decrease in the lattice parameters, which is justified by the results shown in Table 1.

In addition, the diffractogram of $MnO_x/Al_2O_3$ mixed oxides catalysts shows four peaks at 28.70°, 37.28°, 42.78° and 56.70°, indexes of $MnO_2$ crystallization in the form of pyrolusite [22,23]. With the addition of Ce, the intensity of peaks becomes significantly weak and the size of $MnO_2$ particle estimated according to the Scherrer equation, applied for [1 0 1] diffraction, decreases from 16.9 to 7.0 nm (Table 1). For the samples with Mn/Ce ratio less than 1, the reflections of $MnO_2$ almost disappear, due either to the formation of $MnCeO_x$ 'solid solutions' with cubic fluorite structure or to the interaction of Mn species with alumina support [26].

The results of TPR analyzes for $Mn_xCe_y/Al_2O_3$ mixed oxides catalysts are shown in Fig. 2. Two peaks on TPR profiles result from the reduction of Mn ions belonging to different structures/phases. $H_2$-TPR profile on $MnO_x/Al_2O_3$ shows two overlapped strong reduction peaks with maximums at 394 and 468 °C, respectively. Assuming that MnO is the final reduction state [26] from various Mn species in the initial $MnO_x$, it is reasonable to propose that the peak at low temperature could be assigned to the reduction of $MnO_2/Mn_2O_3$ to $Mn_3O_4$, and the one at high temperature, to the combined reduction of $Mn_3O_4$ to MnO [27–29] and surface oxygen removal of ceria. The reduction of $CeO_2/Al_2O_3$ occurs at 547 and 634 °C in the range of experimental temperature, associated with the reduction of surface $Ce^{4+}$ ions [23] and Ce species interacted with $Al_2O_3$, respectively. Moreover, the consumption of $H_2$ is less as compared with the reduction features of $MnO_x/Al_2O_3$, due to small mole value of Ce with the same weight as Mn and small change of electronic valence from $Ce^{4+}$ to $Ce^{3+}$.

For $Mn_8Ce_2/Al_2O_3$ and $Mn_9Ce_1/Al_2O_3$ containing high Mn content, the reduction temperatures systematically shift to lower values. $H_2$-TPR profiles exhibit two broad reduction peaks around 351 and 442 °C, respectively. The former can be related to the presence of "isolated" $Mn^{4+}$ ions which "embedded" into the surface defective positions of the ceria lattice. The latter can be assigned to the reduction of $Mn^{3+}$ species. Their reduction is promoted by a high degree of coordinative unsaturation and, perhaps, by neighboring $Ce^{4+}$ ions, which, in turn, undergo reduction to $Ce^{3+}$ species [30]. Compared with $MnO_x/Al_2O_3$, the consumption of $H_2$ is smaller due to the decrease in the amount of Mn. For $Mn_2Ce_8/Al_2O_3$ and $Mn_5Ce_5/Al_2O_3$ with low content of Mn, the reduction profiles shift gradually to higher temperatures with the decrease in the amount of Mn and even disappear, resulting from the fact that the proportion of Mn species interacted with alumina support increases, leading to difficult reduction of Mn species. The reduction temperature of Ce species on surface shifts from 546 to 536 °C. This phenomenon indicates that the addition of Mn into ceria matrix promotes the dispersion of Ce species so that the reduction of Ce species becomes easy.

Fig. 3 presents XPS measurement of O1s core level of oxygen species on the surface of $Mn_8Ce_2/Al_2O_3$ and $CeO_2/Al_2O_3$ catalysts. The O1s spectrum of $CeO_2$ has two peaks at 531.1 and 530.0 eV, assigned to lattice oxygen, while the O1s core level of lattice oxygen on $Mn_8Ce_2/Al_2O_3$ catalyst is exclusively at 531.7 eV because of "Mn ← O" electron-transfer processes [23], hence leading to the increase of reactivity of lattice oxygen with $H_2$ in $H_2$-TPR, as indicated in Fig. 2. This phenomena is in line with the results obtained by Arena et al. [23], who found that "Mn ← O" electron-transfer processes enable the formation of very reactive electrophilic oxygen species.

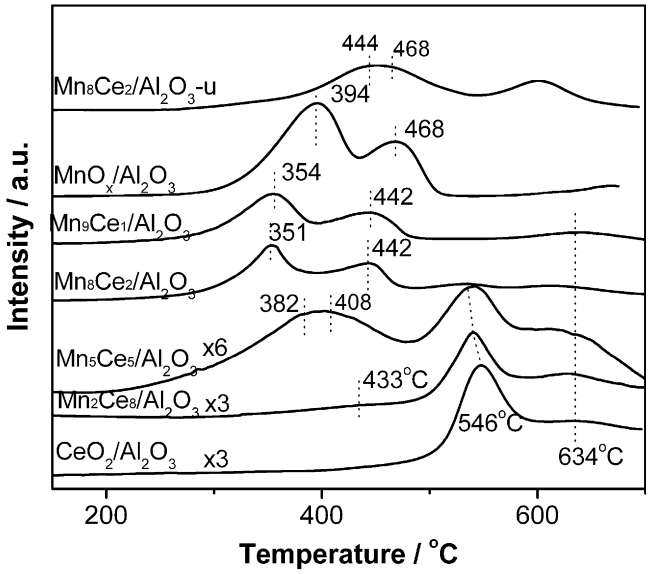


**Fig. 2.** TPR profiles of $Mn_xCe_y/Al_2O_3$ mixed oxides catalysts with different ratios of Mn/Ce; u, the used catalyst.

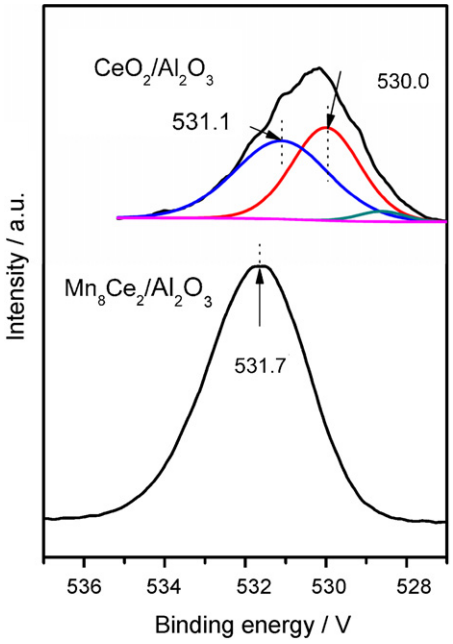


**Fig. 3.** O1s XPS spectra for $Mn_8Ce_2/Al_2O_3$ and $Ce/Al_2O_3$ catalysts.

### 3.2. Activity tests

In order to check whether some reactions under thermal combustion condition could take place, a blank test, with 3 mm crushed quartz glass (40–60 mesh) packed in the reactor, was carried out. As shown in Fig. 4, the conversion of CB without catalyst occurs only above 450 °C to a lower extent; meanwhile Li and co-workers [31] found no significant oxidation of CB at temperature up to 500 °C in a blank reactor experiment. $Al_2O_3$ support is found to exhibit certain activity for CB catalytic combustion, but the conversion is below 70% at 550 °C.

$Mn_xCe_y/Al_2O_3$ mixed oxides catalysts appear to be superior for CB catalytic combustion, of which $Mn_8Ce_2/Al_2O_3$ has the best activity, and its complete combustion temperature ($T_{95\%}$) of CB is as low as 338 °C at GHSV 15,000 ml/g h. With the decrease in Mn content, the activity of $Mn_xCe_y/Al_2O_3$ catalysts reduces. However, for $MnO_x/Al_2O_3$, the conversion of CB at 95% can only be reached at

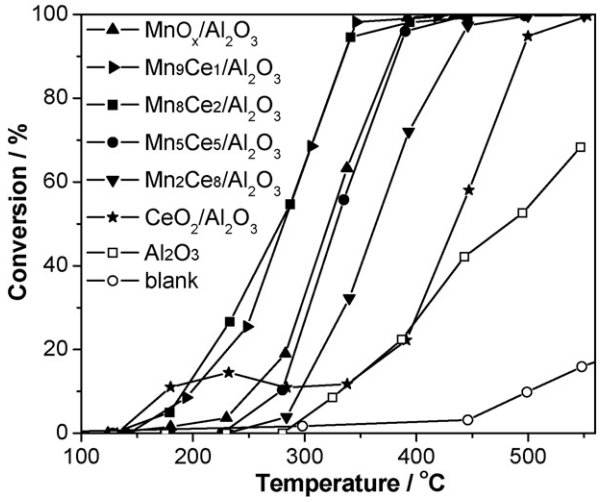


**Fig. 4.** The catalytic activity of over the fresh $Mn_xCe_y/Al_2O_3$ mixed oxides catalysts for CB combustion, gas composition: 1000 ppm CB, 10% $O_2$, $N_2$ balance; GHSV = 15,000 ml/g h.

higher temperature (390 °C). $CeO_2/Al_2O_3$ presents a higher activity than other catalysts under study, but it deactivates slightly from 15% at 230 °C to 11% at 286 °C with the conversion of CB. The conversion increases gradually with the further increase of temperature, and reaches 95% at 502 °C, which is much lower than the temperature for total conversion of CB on the unsupported $CeO_2$ [32]. The incorporation of $MnO_x$ into $CeO_2$ greatly improves the activity and stability, depending on the Mn content. For $Mn_2Ce_8/Al_2O_3$, the temperature which needed for 50% conversion of CB shifts to 361 °C from 433 °C for $CeO_2$. Moreover, the deactivation does not occur over a short time period.

### 3.3. Effect of space velocity on CB catalytic combustion

The catalytic processes for VOCs treatment usually require a gas space velocity (GHSV) varying from 10,000 to 30,000 ml/g h. Table 2 shows the conversion and reaction rate of CB over $Mn_xCe_y/Al_2O_3$ catalysts as a function of GHSV at 300 °C. Both the conversion and reaction rate over $Mn_xCe_y/Al_2O_3$ catalysts with Mn/Ce ratio of 4, 1 and 0.25 decrease with the increase in GHSV, because the average residence time for reactants through the bed decreases and thus high temperature is needed to achieve a sufficient conversion at a higher space velocity. For $Mn_8Ce_2/Al_2O_3$, the conversion of CB at GHSV of 30,000 ml/g h decreases by 46% and 22% as at GHSV of 7500 and 15,000 ml/g h, respectively. In the case of $Mn_2Ce_8/Al_2O_3$, the largest of drop of 90% in the conversion of CB is observed with the increase of GHSV from 7500 to 30,000 ml/g h. This phenomenon may be ascribed to the fact that high GHSV partly enhances the removal of Cl species for $Mn_8Ce_2/Al_2O_3$, even if high content of Cl species on surface due to high conversion.

### 3.4. Effect of inlet reactant concentration on CB catalytic combustion

The effect of inlet CB concentration on the conversion over $Mn_xCe_y/Al_2O_3$ mixed oxides catalysts at the space velocity of 15,000 ml/g h at 300 °C was investigated. It can be seen in Table 2 that the reaction rate has a significant variation with the increase in the inlet CB concentrations from 500 to 2000 ppm, especially for $Mn_8Ce_2/Al_2O_3$ catalyst, which shows more increase in activity at 2000 ppm of CB. With the increase of Ce content, the increase in CB concentration becomes gradually unfavorable to the conversion of CB. Within ±1.5% of the average deviation of CB concentration, the dependence of reaction rate on CB concentration over $Mn_xCe_y/Al_2O_3$ mixed oxides catalysts becomes from positive values at Mn/Ce ratio greater than 1 to negative values at that ratio less than 1, indicating that the adsorption of HCl or $Cl_2$ produced from the decomposition of CB is stronger on the catalyst with high content of Ce. This phenomenon was found in our previous work [32].

To obtain insight of the types of oxygen species to be involved in the reaction, the effect of concentration of oxygen on CB combustion over $Mn_8Ce_2/Al_2O_3$ was investigated. The results obtained when the oxygen concentration varied stepwise or was set at a given value from 0 to 20% are presented in Fig. 5. In the former tests, the activity stability was investigated with different concentrations of oxygen. The change of activities was observed within 60 min at a given oxygen concentration at 350 °C and plotted as conversion of CB vs. oxygen concentration and reaction time. It is interesting to find that $Mn_8Ce_2/Al_2O_3$ presents significant activity in the absence of oxygen. However, this activity decreases gradually, and as the result of it, the conversion falls from 26 to 0% within the reaction duration of 60 min (Fig. 5A). In the next 60 min duration where the oxygen content in the feedstock maintains at the stoichiometric level 0.8%, conversion first increases up to 75% then decreases to 42% at the end of the test. This phenomenon implies that sto-

**Table 2**
The effects of reaction conditions on the activity of catalysts for CB catalytic combustion at 300 °C.

| Catalysts | Space velocity (ml/g h) | | | | | | CB concentration (ppm) | | | | | |
|---|---|---|---|---|---|---|---|---|---|---|---|---|
| | 7500 | | 15,000 | | 30,000 | | 500 | | 1000 | | 2000 | |
| | C (%)[a] | R[b] | C (%) | R | C (%) | R | C (%)[c] | R[d] | C (%) | R | C (%) | R |
| $MnO_x/Al_2O_3$ | 69 | 6.9 | 32 | 3.2 | 18 | 1.8 | 38 | 1.9 | 32 | 3.2 | 21 | 4.2 |
| $Mn_8Ce_2/Al_2O_3$ | 93 | 9.3 | 64 | 6.4 | 50 | 5.0 | 77 | 3.9 | 64 | 6.4 | 37 | 7.4 |
| $Mn_5Ce_5/Al_2O_3$ | 71 | 7.1 | 26 | 2.6 | 13 | 1.3 | 51 | 2.6 | 26 | 2.6 | 16 | 3.6 |
| $Mn_2Ce_8/Al_2O_3$ | 30 | 3.0 | 12 | 1.2 | 3.3 | 0.3 | 35 | 1.8 | 12 | 1.2 | 4.4 | 0.9 |
| $CeO_2/Al_2O_3$ | 14 | 1.4 | 3.3 | 0.3 | NT | | 15 | 0.8 | 3.3 | 0.3 | NT | |

[a] The conversion (%) of CB.
[b] The reaction rate (μmol/$g_{cat}$ min) at 300 °C in the reaction feed with 1000 ppm CB, 10% $O_2$, $N_2$ balance.
[c] The conversion of CB.
[d] The reaction rate (μmol/$g_{cat}$ min) at 300 °C in the reaction feed 10% $O_2$, $N_2$ balance, at 15,000 ml/g h. NT, not detectable.

ichiometric amount of oxygen is deficient for the demand from the reaction. In the following tests, each lasting 60 min, the oxygen levels gradually increase, and together with this increase, conversions are improved. For example, conversion only varies from 52 to 48% in the test where oxygen level becomes 7.2%. In the last test, conversion keeps 52% as the oxygen level reaches 20%. Considering the big difference of conversions within the test duration, e.g., from 72 to 42%, decrease in the activity of $Mn_8Ce_2/Al_2O_3$ could be due to the poisoning of Cl. With the mode of raising temperature, the conversion of CB in free-oxygen stream increases rapidly at 400 °C and reaches 90% at 520 °C (Fig. 5B). The analysis of products shows that there are $CO_2$ and HCl in the effluent before 400 °C. The color of used $Mn_8Ce_2/Al_2O_3$ is olive drab, as the same as that of the sample after TPR. XPS spectrum presents the binding energy of Mn species at 641.0 eV, indicating that Mn species was reduced to $Mn^{2+}$ ions during the reaction in the free-oxygen stream. In other words, the lattice oxygen participates in oxidation of CB. Changing the concentration of oxygen from 0.8 (stoichiometric) to 20% (largely excessive), the conversion curve of CB shifts 40 °C lower in the temperature, that is to say, the dependence of rate on oxygen concentration is weak. This phenomenon indicates that the transform of gas oxygen into the lattice oxygen is rapid. Considering TPR results, $Mn_8Ce_2/Al_2O_3$ catalyst can be reduced at lower temperature than other catalysts, and a high activity of $Mn_8Ce_2/Al_2O_3$ catalyst in the low oxygen concentration or in the absence of oxygen can be ascribed to its high re-oxidation ability which plays a important role in CB oxidation. At high temperature, especially higher than 430 °C, the conversion of CB is mainly dependent on the decomposition process. It could be concluded that the dechlorination can occur over $Mn_8Ce_2/Al_2O_3$ catalyst.

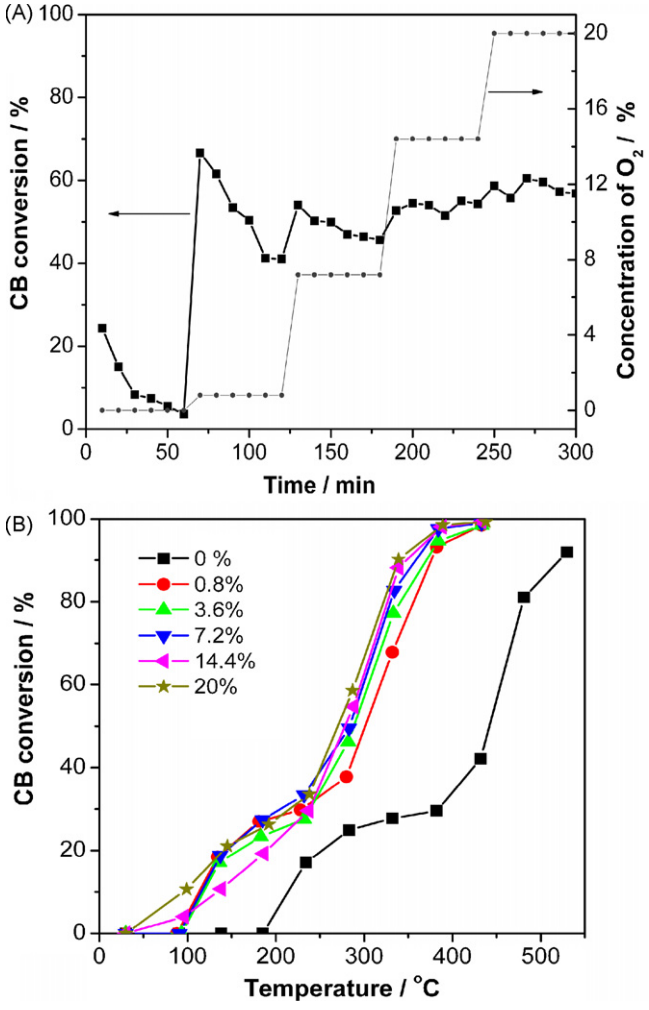


**Fig. 5.** The effect of oxygen concentration on the activity of $Mn_8Ce_2/Al_2O_3$ catalyst for CB combustion, CB 1000 ppm, $N_2$ balance; GHSV = 15,000 ml/g h: (A) oxygen concentration was varied stepwise at 350 °C; (B) oxygen concentration was set at a given value.

### 3.5. The analyzes of products

Within the limit of FID, all the catalysts studied in this experiment provide more than 99.5% selectivity to carbon oxides (more than 98% $CO_2$ and trace CO) and no other C-containing by-products are detected. This is very different from the results from the employment of noble metal-based catalysts in the tests [31,33,34], where substantial amount of polychlorinated benzene are formed during catalytic combustion of CB. The Cl balance reaches 80–85%, that means that the deposition of Cl species on the surface of catalysts occurs.

### 3.6. Catalyst deactivation

For the catalytic combustion of CVOCs, the catalyst deactivation is still a hurdle in commercial applications. In previous work, $CeO_2$ was found to rapid deactivation due to strong adsorption of Cl on active sites during the catalytic combustion of trichloroethylene [9,35]. Therefore it is necessary to investigate the stability of $Mn_8Ce_2/Al_2O_3$, $MnO_x/Al_2O_3$ and $CeO_2/Al_2O_3$ catalysts was investigated in the CB combustion. The results from the activity tests with stepwise variations in the temperature are presented in Fig. 6. In these activity tests, the activity stability was studied at different temperatures, that is, the change of activities was observed with every 60 min at a given temperature and plotted as conversion of CB vs. the reaction temperature and reaction time. During the test, the activity of every catalyst was evaluated with a step by step temperature from 50 to 500 °C.

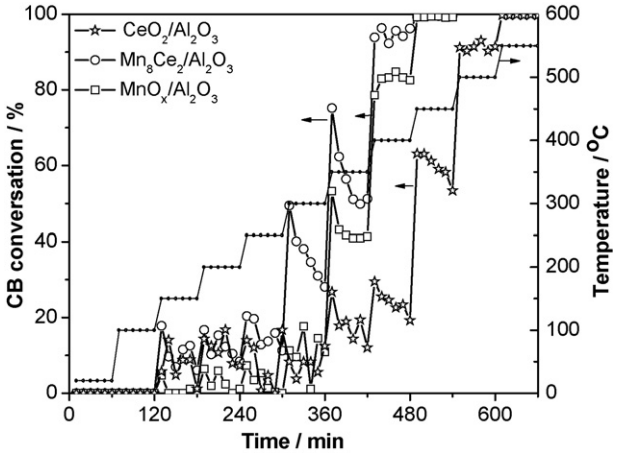


**Fig. 6.** The stability of catalysts for CB oxidation at different temperature, gas composition: 1000 ppm CB, 10% $O_2$, $N_2$ balance; GHSV = 15,000 ml/g h.

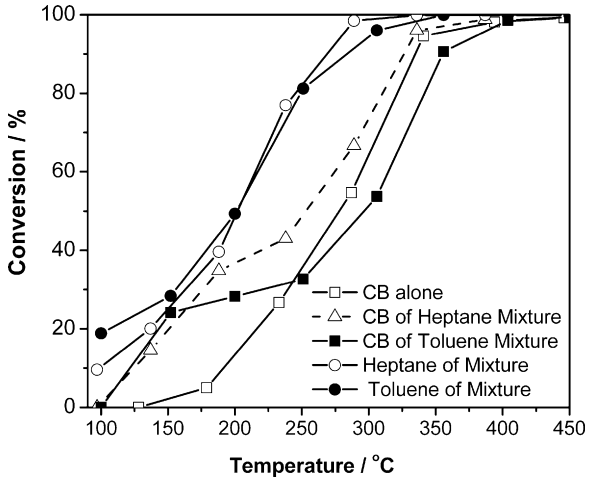


**Fig. 7.** The activity of $Mn_8Ce_2/Al_2O_3$, CB alone: 1000 ppm CB; mixture: 1000 ppm CB + 1000 ppm heptane or toluene; 10% $O_2$, $N_2$ balance; GHSV = 15,000 ml/g h.

As shown, $CeO_2/Al_2O_3$ presents an unstable activity until 500 °C at which stable activity is observed without a substantial decrease in conversion. However, in the case of $MnO_x/Al_2O_3$, there is not a significant drop in the activity observed, although it shows fairly low activity in 100–300 °C. As for the combination of $MnO_x$ with $CeO_2$, the activity of $Mn_8Ce_2/Al_2O_3$ really promotes on the various temperature steps, but its activity is not stable until 400 °C, at which $Mn_8Ce_2/Al_2O_3$ achieves a high stable activity without any decrease in conversion.

For practical use, it is necessary to test the stability at 400 °C for in a long duration. It can be found that the stable activity can be achieved within 0.5–1 h over both catalysts, $Mn_8Ce_2/Al_2O_3$ and $CeO_2/Al_2O_3$, on which the stable conversion of CB within 20 h maintains at about 90% and 20%, respectively. Because of the sharp activity drop of $CeO_2/Al_2O_3$ in the tests, the deactivation of $Mn_8Ce_2/Al_2O_3$ during the combustion of CB can be considered as the poisoning of Ce species, probably due to the strong adsorption of HCl or $Cl_2$ produced from the combustion of CB on the $CeO_2$ surface to result in the blockade of active sites [9,35]. Ce species with high dispersion possesses a large amount of active oxygen which can promote the removal of chlorine from Ce species [32]. Therefore, $Mn_8Ce_2/Al_2O_3$, with a smaller size of cerianite (see Table 1) can dechlorinate at lower temperature than $CeO_2/Al_2O_3$ does, on which, the removal of chlorine becomes evident only higher than 500 °C.

Van den Brink reported that hydrocarbon could remove Cl species from the surface of Pt catalysts [36,37]. In this work, the effects of heptane or toluene in the reaction mixture on the activity and stability were investigated. It can be seen in Fig. 7 that the conversion of CB in binary mixture with heptane or toluene on $Mn_8Ce_2/Al_2O_3$ increases significantly at low temperature, and the temperature needed for 26% conversion shifts from 227 to 160 °C. The reaction pathway may involve a H-atom abstraction from heptane or toluene onto $Mn_8Ce_2/Al_2O_3$, and this H species is reactive for the combination with the adsorbed Cl species to form HCl. Van den Brink et al. described this process in the catalytic combustion of CB on $Pt/Al_2O_3$ [36]. With raising temperature, this effect due to the addition of heptane decreases gradually, and the added toluene even decreases slightly the conversion of CB, indicating that the consumption of surface oxygen in the oxidation of heptane or toluene decreases oxygen species necessary to remove the adsorbed Cl species. In the run at high GHSV of 30,000 ml/g h, it was found that the conversion curve of CB shifts to low temperature by 50 °C. It can be deduced that the removal of the strongly adsorbed Cl species is difficult at low temperature because oxygen species may be not active enough to react with Cl species, but can be promoted by hydrogen species from the hydrocarbon.

The physico-chemical properties of the used catalysts were characterized. The results show that after used for the combustion of CB for 500 min at 350 °C, the specific surface area of $Mn_xCe_y/Al_2O_3$ catalysts rarely change, no phase transformation was observed in their XRD patterns and the obvious deposit of coke on the catalyst surface was not detected by TG techniques. However, the change of XPS spectra of surface species was observed. XPS spectrum of the used $Mn_8Ce_2/Al_2O_3$ shows Cl 2p peak at 198.0 eV and 0.34 at.% of Cl species while for $Mn_2Ce_8/Al_2O_3$ at 198.6 eV with 0.80 at.% of Cl. This results show that more Cl species on $Mn_2Ce_8/Al_2O_3$ is ascribed to stronger adsorption of Cl species. Due to the deposition of Cl species [34], the reduction temperature of Mn species will increase, but the employed temperature varies with the change in the Ce/Ce + Mn ratio. Reduction temperature for the used $Mn_8Ce_2/Al_2O_3$ is lower than that of used $Mn_2Ce_8/Al_2O_3$ (Fig. 2). In other words, better reducibility of $Mn_xCe_y/Al_2O_3$ catalyst mixed oxides makes surface possess more available lattice oxygen to exchange chloride species produced during the reaction.

Considering the continuous production of HCl and $Cl_2$ in the process of CB combustion, the chlorination of Ce and Mn species in the used catalysts was investigated by Raman spectra. The Raman spectrum (not shown) indicates that, the bands at 177,208 $cm^{-1}$ ($CeCl_3$), 119,327 $cm^{-1}$ (CeOCl) [38] and 1600 $cm^{-1}$ ($MnO_xCl_y$, $MnCl_2$) [39] are not observed. It is suggested that the chlorination of Ce and Mn species under the reaction condition (the excess of $O_2$) proceeds so difficultly, or the oxidation of chlorinated Mn or Ce species proceeds so rapidly that the amount of chlorinated Mn or Ce is very small.

## 4. Conclusion

A series of $Mn_xCe_y/Al_2O_3$ mixed oxides catalysts with different compositions prepared by wet impregnation method were tested for catalytic combustion of chlorobenzene (CB). $Mn_8Ce_2/Al_2O_3$ catalyst is identified as the most active catalyst, on which the temperature of complete combustion of CB is 338 °C. The main products from CB catalytic destruction over the $Mn_xCe_y/Al_2O_3$ catalysts are HCl, $Cl_2$, $CO_2$ and trace amount of CO, and polychlorinated compounds have not been detected. $Mn_xCe_y/Al_2O_3$ mixed oxides catalysts with high Mn/Ce ratios present a stable high activity, which is related to their better reducibility. The characterization of catalysts confirms that the reducibility of catalysts is dependent

on the interaction of Ce species with Mn species within the solid solution with cerianite.

## Acknowledgements

We would like to acknowledge the financial support from National Basic Research Program of China (No. 2010CB732300), National Natural Science Foundation of China (No. 20977029) and the Commission of Science and Technology of Shanghai Municipality (0852nm00900).

## References

[1] Abbas Khaleel, Aysha Al-Nayli, Appl. Catal. B: Environ. 80 (2008) 176.
[2] M. Taralunga, B. Innocent, J. Mijoin, P. Magnoux, Appl. Catal. B: Environ. 75 (2007) 139.
[3] Beatriz Miranda, Eva Díaz, Salvador Ordóñez, Fernando V. Díez, Catal. Commun. 7 (2006) 945.
[4] F. Bertinchamps, M. Treinen, P. Eloy, A.M. Dos Santos, M.M. Mestdagh, E.M. Gaigneaux, Appl. Catal. B: Environ. 70 (2007) 360.
[5] F. Bertinchamps, C. Gregoire, E.M. Gaigneaux, Appl. Catal. B: Environ. 66 (2006) 1.
[6] M. Taralunga, J. Mijoin, P. Magnoux, Catal. Commun. 7 (2006) 115.
[7] M. Guillemot, J. Mijoin, S. Mignard, P. Magnoux, Appl. Catal. A: Gen. 327 (2007) 211.
[8] Q.G. Dai, X.Y. Wang, G.Z. Lu, Catal. Commun. 8 (2007) 1645.
[9] Q.G. Dai, X.Y. Wang, G.Z. Lu, Appl. Catal. B: Environ. 81 (2008) 192.
[10] M. Magureanu, N.B. Mandache, J. Hu, R. Richards, M. Florea, V.I. Parvulescu, Appl. Catal. B: Environ. 76 (2007) 275.
[11] M. Guillemot, J. Mijoin, P. Magnoux, Appl. Catal. B: Environ. 75 (2007) 249.
[12] Beatriz de Rivas, Rubén López-Fonseca, Carmen Sampedro, I. José, Gutiérrez-Ortiz, Appl. Catal. B: Environ. 90 (2009) 545.
[13] R. López-Fonseca, B. de Rivas, J.I. Gutiérrez-Ortiz, A. Aranzabal, J.R. González-Velasco, Appl. Catal. B: Environ. 41 (2003) 31.
[14] X.T. Sayle, D. Sayle, Phys. Chem. Chem. Phys. 7 (2005) 2936.
[15] M.C. Álvarez-Galván, V.A. de la Peña O'Shea, J.L.G. Fierro, P.L. Arias, Catal. Commun. 4 (2003) 223.
[16] C.N. Costa, V.N. Stathopoulos, V.C. Belessi, A.M. Efstathiou, J. Catal. 197 (2001) 350.
[17] R. Craciun, B. Nentwich, K. Hadjiivanou, H. Knözinger, Appl. Catal. A: Gen. 243 (2003) 67.
[18] G. Qi, R.T. Yang, J. Phys. Chem. B 108 (2004) 15738.
[19] M. Kramer, W.F. Maier, Appl. Catal. A: Gen. 302 (2006) 257.
[20] J.R. González-Velasco, A. Aranzabal, R. López-Fonseca, R. Ferret, J.A. González-Marcos, Appl. Catal. B: Environ. 24 (2000) 33.
[21] R. López-Fonseca, A. Aranzabal, J.I. Gutiérrez-Ortiz, J.I. Álvarez-Uriarte, J.R. González-Velasco, Appl. Catal. B: Environ. 30 (2001) 303.
[22] F. Arena, E. Alongi, P. Famulari, A. Parmaliana, G. Trunfio, Catal. Lett. 107 (2006) 39.
[23] F. Arena, G. Trunfio, J. Negro, B. Fazio, L. Spadaro, Chem. Mater. 19 (2007) 2269.
[24] M. Machida, M. Uto, D. Kurogi, T. Kijima, Chem. Mater. 12 (2000) 3158.
[25] D. Terribile, A. Trovarelli, C. De Leitenburg, A. Primavera, G. Dolcetti, Catal. Today 47 (1999) 133.
[26] F. Kapteijn, L. Singoredjo, A. Andreini, Appl. Catal. B: Environ. 3 (1994) 173.
[27] F. Arena, T. Torre, C. Raimondo, A. Parmaliana, Phys. Chem. Chem. Phys. 3 (2001) 1911.
[28] J. Carnö, M. Ferrandon, E. Björnbom, S. Järås, Appl. Catal. A: Gen. 155 (1997) 265.
[29] J. Trawczyński, B. Bielak, W. Mišta, Appl. Catal. B: Environ. 55 (2005) 277.
[30] S.T. Hussain, A. Sayari, F. Larachi, Appl. Catal. B: Environ. 34 (2001) 1.
[31] Y. Liu, Z. Wei, Z. Feng, M. Luo, P. Yang, C. Li, J. Catal. 202 (2001) 200.
[32] X.Y. Wang, Q. Kang, D. Li, Appl. Catal. B: Environ. 86 (2009) 166.
[33] A. Musialik-Piotrowska, B. Mendyka, Catal. Today 90 (2004) 139.
[34] R.W. van den Brink, P. Mulder, R. Louw, Catal. Today 54 (1999) 101.
[35] Xingyi Wang, Qian Kang, Dao Li, Catal. Commun. 9 (2008) 2158.
[36] R.W. van den Brink, R. Louw, P. Mulder, Appl. Catal. B: Environ. 25 (2000) 229.
[37] F. Arena, P. Famulari, N. Interdonato, G. Bonura, F. Frusteri, L. Spadaro, Catal. Today 116 (2006) 384.
[38] R.M. Lago, M.L.H. Green, S.C. Tsang, M. Odlyha, Appl. Catal. B: Environ. 8 (1996) 107.
[39] D. Sarmeo, S. Blazewicz, M. Mermoux, P. Touzain, Carbon 39 (2001) 2049.